Automatika
Journal for Control, Measurement, Electronics, Computing and Communications

ISSN: (Print) (Online) Journal homepage: www.tandfonline.com/journals/taut20

Optimal design of automatic generation control based on BBPSO-tuned PI for a restructured environment

P. M. Karthikeyan & S. Baghya Shree

To cite this article: P. M. Karthikeyan & S. Baghya Shree (2024) Optimal design of automatic generation control based on BBPSO-tuned PI for a restructured environment, Automatika, 65:3, 925-934, DOI: 10.1080/00051144.2024.2325314

To link to this article: https://doi.org/10.1080/00051144.2024.2325314

Published online: 11 Mar 2024.

AUTOMATIKA
2024, VOL. 65, NO. 3, 925–934
https://doi.org/10.1080/00051144.2024.2325314

Optimal design of automatic generation control based on BBPSO-tuned PI for a restructured environment

P. M. Karthikeyan[a] and S. Baghya Shree[b]

[a]Department of Electrical and Electronics Engineering, Anna University, Chennai, India; [b]Department of Electrical and Electronics Engineering, Anna University Regional Campus, Madurai, India

ABSTRACT
This paper intends to model an AGC regulator for a restructured environment using Bare Bone Particle Swarm Optimization (BBPSO). The gain-controlled Proportional–Integral (PI) Controller is designed here to enhance the performance of the BBPSO algorithm along with Gaussian distribution. The practical difficulty in handling the area control error to zero is the sudden variations in load. In practice, the tremendous contribution of deregulation in the power sector causes volatility in frequency and tie-line power deviations. To ensure the robustness of the proposed controller, three different cases of power system transactions have been considered. The performance has been validated by comparing it with Real Coded Genetic Algorithm-tuned PI controller (RCGA-PI) and Differential Evolutionary Algorithm-tuned PI controller (DE-PI) for the five area Thermal-Thermal generation test system. Moreover, the dynamic performance of an extensive range of demands and disturbances of all areas like settling time and overshoot against parametric precariousness has been done on the proposed test system.

ARTICLE HISTORY
Received 24 November 2023
Accepted 26 February 2024

KEYWORDS
AGC; deregulated power system; BBPSO-tuned PI controller; GRC

1. Introduction

Automatic Generation Control (AGC) is vital to retaining the scheduled values in the interconnected large-area power system as far as the frequency and tie-line power are concerned. A restructured power system is a complex model which constitutes various uncertainties and sudden load perturbations. The intention of AGC is to adjust the output of many generators at diverse power plants, in response to changes in the load. Because the grid requires that generation and load closely balance instant to instant, the regular tuning of power generations is essential and it can be reviewed by frequency and tie-line power flows. Moreover, the electricity market reformed from a regular Vertical Integrated utility to the restructured system and hence this article concentrates on AGC in a deregulated environment. The deregulated power market is an open market and power generating authorities are categorized as Gencos, Distribution authorities as Discos and Transmission network bodies as Transcos; however, the coordination between those bodies is being taken care of by Independent System Operator (ISO). Furthermore, each component exhibits its role in executing the rules and economic incentives which has been set by the government for driving the power industry. This power environment gives autonomy to Discos to transact with any gencos as per their contract and those transactions have been monitored and controlled through ISO. Many researchers over the decades have proposed control strategies for achieving the motto of AGC.

The study of secondary controllers for automatic generation control (AGC) is done and analysis is performed for frequency and power control. The performance in the two-area system reveals that cascaded controllers show minimum deviations [1]. AGC of a two-area four-unit interconnected thermal power system has been performed with the differential evolution particle swarm optimization technique (DEPSO). Results with DEPSO-tuned three differential PID controllers have been evaluated [2]. Five different controller structures tuned by the ERWCA optimization technique are employed for AGC. The reliability of power system operation is evaluated by comparing the models [3]. The performance comparison has been made for AGC of an interconnected hydro-thermal system between hybrid neuro-fuzzy, fuzzy and integral controllers [4]. Many controlling techniques are employed for AGC. The performance of the fuzzy controller is compared with the PI controller for a two-area system. Simulation results reveal better activity on the fuzzy controller [5]. Renewable energy resources are employed to meet the increasing load demands. For a multi-source power system, gain tuned proportional integral derivative controller with a filter (F-PID-N) is recommended through a fuzzy approach. The robustness of the controller is proved

CONTACT S. Baghya Shree baghya_shree@yahoo.com Department of Electrical and Electronics Engineering, Anna university Regional Campus Madurai, Tamilnadu, India-625019

by changing system parameters. Renewable energy sources are pollution-free, eco-friendly and more reliable. Uninterrupted power supply can be met with these sources. The controller for AGC with renewable energy sources is yet to be developed. A novel cascaded PID controller is developed for five equal area systems with non-linearities and the simulation result provides the superiority of the controller [6]. the power system is complex. It consists of multiple areas inter-connected and need to be energized by electrical energy. A single source of electrical energy cannot be met out of the same, and so a multi-source power system is employed. An enhanced whale optimization algorithm was proposed for AGC [7]. The Internet of Things (IoT) is a modern powerful tool to simplify complexity. In AGC random disturbances need to be carefully evaluated and with the help of IoT the complexity can be easily handled and optimal control can be done efficiently [8]. Differential evolution (DE) optimization technique-tuned TDOFPID for AGC is developed. The performance is validated through DE optimization and also through Interline power flow control (IPFC). Both give better responses. Stable frequency maintenance in the multi-area power system is one of the chaotic tasks. In this, a three-area interconnected power system is designed with an Integral controller and PID controller for AGC. Simulation results were compared for these models [9]. Solar photovoltaic power generation is a milestone in renewable power generation. However, it has poor control performance and is not suited for general application. To improve it, AGC is developed based on the adaptive PID control algorithm. The findings reveal that it has the advantage of high control accuracy and fast response [10]. Barebone PSO, Gaussian sampling has been employed to improve particle position and purge the exploit of velocity [11]. The application of the suggested FO-PI controllers based on PSO presents enhancement in the dynamic frequency response performance of the SEPS according to ROCOF, Settling Time, Maximum Overshoot, Nadir and well damping in a wide range of operating conditions. Even the existence of Generating Rate Constraints (GRC)confirms its strength [12]. The simulation results obtained from the series connected PI-PDF and CPI-PDF are found better than other controllers with respect to settling time, rise time, peak value and peak time. The gain is optimized using a differential algorithm [13].

It is essential to design a controller which should handle sudden load demands uncertainties, frequency and inter-area power deviations in tie-line to maintain steady state error as almost null. This article proposes a BBPSO algorithm for tuning the gains of a PI controller for achieving the goals of AGC with Generation Rate Constraint (GRC). The performance of gain-tuned PI through RCGA and DE optimization algorithms was also simulated to compare the performance of the proposed algorithm. Here, five control area models are considered, every area consists of different combinations of thermal reheat and non-reheat turbines. The control area is assumed to be non-uniform in nature (i.e.) area 1 includes three Gencos with one reheat and two non-reheat turbines and two Discos, area 2 with two Gencos with reheat and non-reheat turbine combination and one Disco, area 3 with two Gencos in a combination of two non-reheat turbines and two Discos, area 4 with two Gencos of two reheat turbines and one Disco and area 5 incorporated with two Gencos of two non-reheat turbines and two Discos as illustrated in Figure 1. The Gencos parameters and their control parameters are presented in Tables 1 and 2.

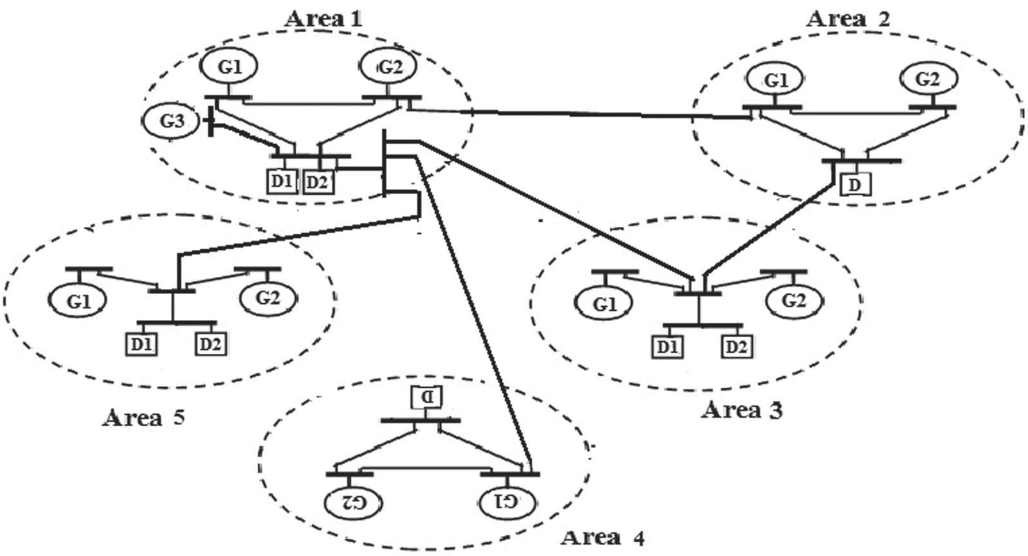

Figure 1. Five-area deregulated power system structure.

Table 1. Genco's parameters.

MVA $_{base}$ (1000 MW) Parameter	Gencos (*k* in area *i*)										
	1-1	2-1	3-1	1-2	2-2	1-3	2-3	1-4	2-4	1-5	2-5
Rate (MW)	900	1000	800	1100	900	1000	1020	850	1050	1000	1020
T_T (S)	0.36	0.42	0.43	0.44	0.4	0.36	0.4	0.38	0.4	0.43	0.36
T_G (S)	0.06	0.07	0.06	0.06	0.08	0.07	0.08	0.085	0.085	0.06	0.08
R (Hz/pu)	2.39	3.3	2.6	2.5	2.39	3	2.39	2	2.39	2.39	2.39
Alpha	0.35	0.3	0.35	0.6	0.4	0.5	0.5	0.5	0.5	0.5	0.5

Table 2. Control parameters.

Parameters	Area				
	1	2	3	4	5
K_P	120	115	125	115	122.5
T_P	20	25	20	25	25
B	0.425	0.385	0.359	0.359	0.433

Note: T_{12} – 0.249pu/Hz; T_{13} – 0.125 pu/Hz; T_{14} – 0.109 pu/Hz; T_{15} – 0.219 pu/Hz; T_{23} – 0.175 pu/Hz.

2. Problem formulation

The control area with different combinations of Discos and Gencos of thermal plants is modelled for the proposed controller. For this deregulated environment, Disco can deal with any Gencos in the control area through the Contract which has been monitored through ISO.

The Area Control Error [13] for the *i*th area [14]

$$\mathrm{ACE}_i = \sum_j (\Delta P_{tie,i,j} + b_i \Delta f_i) \tag{1}$$

where b_i is the frequency bias coefficient of the *i*th area, Δf_i is the frequency error of the *i*th area, $\Delta P_{tie,i,j}$ is the tie-line power flow error between the *i*th area and jth area.

The generation rate has been tuned by the value of ACE based on the demand in a control area. ACE plays a vital role in sustaining the frequency and tie-line power flows to scheduled value [15,16]. Disco Participation Matrix (DPM) shows the activity of Gencos with corresponding Discos, in DPM, the number of rows and columns is equal to the number of Gencos and Discos participated in the contract, respectively. Entry of the matrix reveals a fraction of the total load power contracted by a Disco towards a Genco. The sum of entries in a column is equal to one (i.e.) $\sum cpfij = 1$. The following shows the DPM for the nth area power system:

$$\mathrm{DPM} = \begin{pmatrix} cpf_{11} & cpf_{12} & \cdots & cpf_{1n} \\ cpf_{21} & cpf_{22} & \cdots & cpf_{2n} \\ \vdots & \vdots & \cdots & \vdots \\ cpf_{n1} & cpf_{n2} & & cpf_{nn} \end{pmatrix} \tag{2}$$

$$\mathrm{AGPM} = \begin{pmatrix} \mathrm{AGPM}_{11} & .. & \mathrm{AGPM}_{1N} \\ : & : & : \\ \mathrm{AGPM}_{N1} & .. & \mathrm{AGPM}_{NN} \end{pmatrix} \tag{3}$$

where

$$\mathrm{AGPM}_{ij} = \begin{pmatrix} gpf_{(si+1)(zj+1)} & .. & gpf_{(si+1)(zj+mj)} \\ : & : & : \\ gpf_{(si+ni)(zj+1)} & .. & gpf_{(si+ni)(zj+mj)} \end{pmatrix}$$

For $i,j = 1,2,\ldots, N$, and $s_i = \sum_{k=1}^{i-1} n_i$; $z_j = \sum_{k=1}^{j-1} m_j; s_1 = z_1 = 0$.

where n_i and m_j are the number of Gencos and Discos in area *i* and gpf_{ij} refers to "Generation Participation Factor" and shows the participation factor $\mathrm{Genco_i}$ in total load following the requirement of $\mathrm{Disco_j}$ based on the possible contract. The Sum of all entries in each column of (the Augmented Generation Participation Matrix) AGPM is unity.

GPF reveals the contribution of $\mathrm{Genco_i}$ to $\mathrm{Disco_j}$'s demands based on the possible contract. The addition of all entries in each column of the Augmented Generation Participation Matrix (AGPM) should be one.

The scheduled contracted power exchange is given by

$$\Delta P_{tie12}^{scheduled} = \text{Demand of Discos in area 2 from Gencos in area 1)} - \text{(Demand of Discos in area 1 from Gencos in area 2)}$$

$$d_i = \Delta P_{loc,i} + \Delta P_{di} \tag{4}$$

where

$$\Delta P_{loc,i} = \sum_{j=1}^{mi} \Delta P_{Lj-i};\ \Delta P_{d,i} = \sum_{j=1}^{mj} \Delta P_{ULj-i}$$

$$\eta_i = \sum_{\substack{j=1 \\ j\neq i}}^{N} T_{ij}\Delta f_j, \tag{5}$$

$$\xi_i = \Delta P_{tie,ik,sch} \sum_{\substack{k=1 \\ k\neq i}}^{mj} \Delta P_{tie,ik,sch}, \tag{6}$$

$$\Delta P_{tie,ik,sch} = \sum\nolimits_{j=1}^{ni} \sum\nolimits_{t=1}^{mk} apf_{(si+j)(zk+t)} \Delta P_{Lt-k} - \sum\nolimits_{t-1}^{nk} \sum\nolimits_{j=1}^{mi} apf_{(sk+t)(zi+j)} \Delta P_{Lj-l} \tag{7}$$

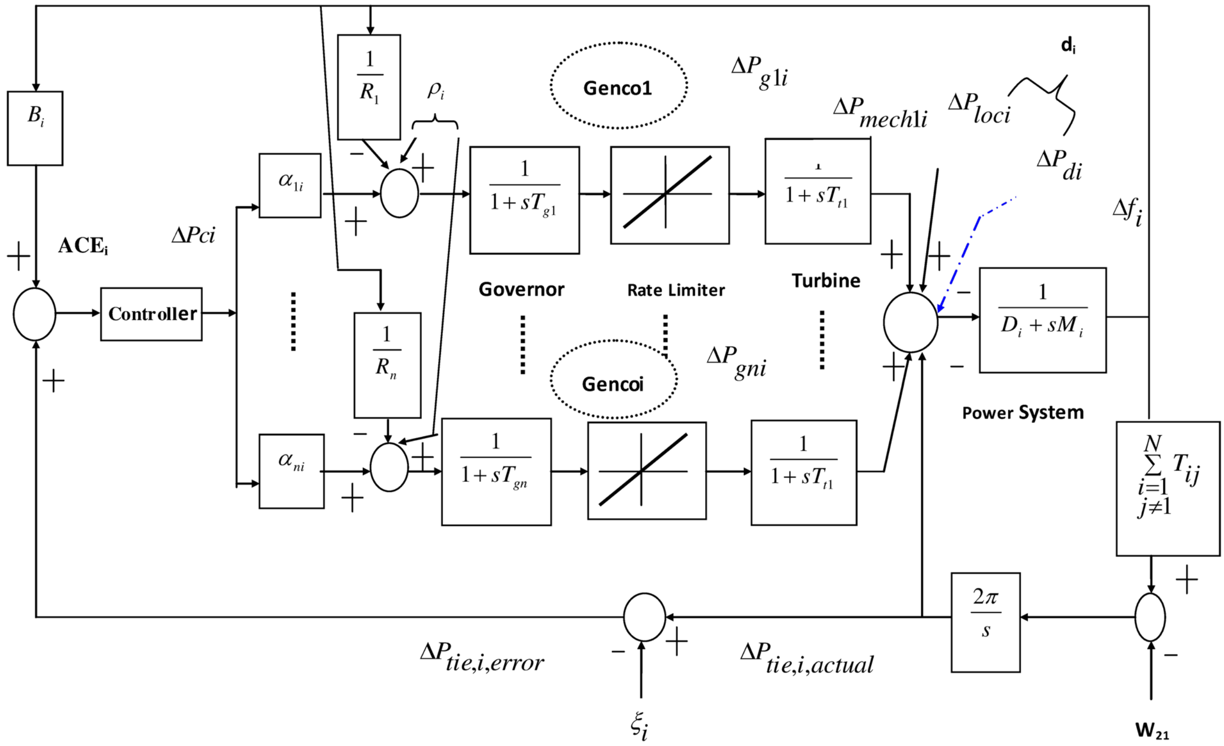

Figure 2. Control area arrangement for the *i*th area with generation rate constraint.

$$\Delta P_{tie,i,error} = \Delta P_{tie,i-actual} - \xi_i \tag{8}$$

$$\rho_i = [\rho_{1i} \ldots . \rho_{ki} \ldots . \rho_{nii}]^T$$

$$\rho_{ki} = \sum\nolimits_{j=1}^{N} \left[\sum\nolimits_{t=1}^{mj} gpf_{(si+k)(zj+t)} \Delta P_{Lt-j} \right]^T \tag{9}$$

$$\Delta P_{m,k-i} = P_{ki} + apf_{ki} \sum_{j=1}^{mj} \Delta P_{ULj-i} \tag{10}$$

where $k = 1,2,\ldots, n_i$.

To put off the excessive control action in power generation between the control areas, generation rate constraint (GRC) (Figure 2) with the nominal value of the GRC (thermal unit) of 3%/min, i.e.$\Delta PG(t) \leq 0.005$p.u.MW/s is considered with the limit bounds of ± 0.0005.

3. BBPSO-PI controller for AGC

The AGC for multi-area generation system is computed through the Proportional–Integral (PI) controller. Even though the conventional methods such as Proportional–Integral Derivative (PID) and state feedback controllers provide zero steady-state deviation [17], they exhibit poor dynamic response and they are time-consuming [18]. The control vector for the PI controller is given by

$$U_i = -[K_{pi} + ACE_i + K_{Ii} \smallint ACE_i dt] \tag{11}$$

where K_{pi} and K_{ii} are the proportional and integral gains of the PI controller

The ACE is used as a control signal in the PI controller and the same has been fed to the governor set point in each area.

3.1. Barebone particle swarm optimization

Barebone PSO (BBPSO) is a scholastic approach for optimizing multi-objective problems. Here, the Gaussian sampling method is preferred for generating new positions of particles. Since it eradicates the velocity term of the conventional PSO algorithm, this strategy does not need to optimize another D-dimensional vector (the velocity component); however; there is no delay as an adaptation is required and while it arises, which could potentially improve the performance. A particle energetically normalizes its velocity to generate a new position in the search space as follows:

$$\text{Vi(t + 1)} = \text{w Vi(t)} = \text{c1r1(pbest} - \text{Xi(t)} + \text{c2r2(gbest} - \text{Xi(t))} \tag{12}$$

$$Xi(t+1) = Xi(t) + Vi(t+1) \tag{13}$$

where Xi and Vi are the position and velocity vector for the ith particle, respectively; pbest is the previous best particle of the ith particle and gbest is the global best particle; r1 and r2 are two independently generated random numbers within [0,1]. The parameter w is known as inertia weight; c1 and c2 are acceleration coefficients.

A new position is updated by Gaussian sampling as follows:

$$Xi(t+1) = N\left(\frac{gbest + pbest}{2}, |gbest - pbest|\right) \tag{14}$$

where $N(.)$ indicates the Gaussian distribution with mean $\frac{gbest+pbest}{2}$ and standard deviation $|gbest - pbest|$

3.2. Pseudo code

Step 1: Choose the number of iterations as 100 and the population size as 20.

Step 2: Generate randomly, "n" particles for gains and frequency biases with uniform probability over the optimized parameter search space $[x_{\min}, x_{\max}]$, similarly, generate initial velocities of all particles, *Vi*.

Step 3: Run the AGC simulink model and enumerate the performance criterion (fitness function) for each particle (Equation 16) at the kth iteration.

Step 4: Calculate the gbest value and the pbest value.

Step 5: Calculate fitness function at gbest and pbest solution.

Step 6: Calculate $Vi(t+1)$ (Equation 12), $Xi(t+1)$ (Equation 13)

Step 7: Update velocity.

Step 8: The position of each particle has to be updated based on updated velocity and the particles are aligned to new positions according to Equation 14. Set

Table 3. Fitness (ITAE) value comparison.

	SCENARIO					
	1		2		3	
Controllers	Fitness value	Computational time (msec)	Fitness value	Computational time (msec)	Fitness value	Computational time (msec)
BBPSO-PI	0.149	0.18	0.226	0.2	0.2331	0.18
RCGA-PI	0.167	0.23	0.137	0.3	0.107	0.23
DE-PI	0.11	0.3	0.13	0.35	0.156	0.3

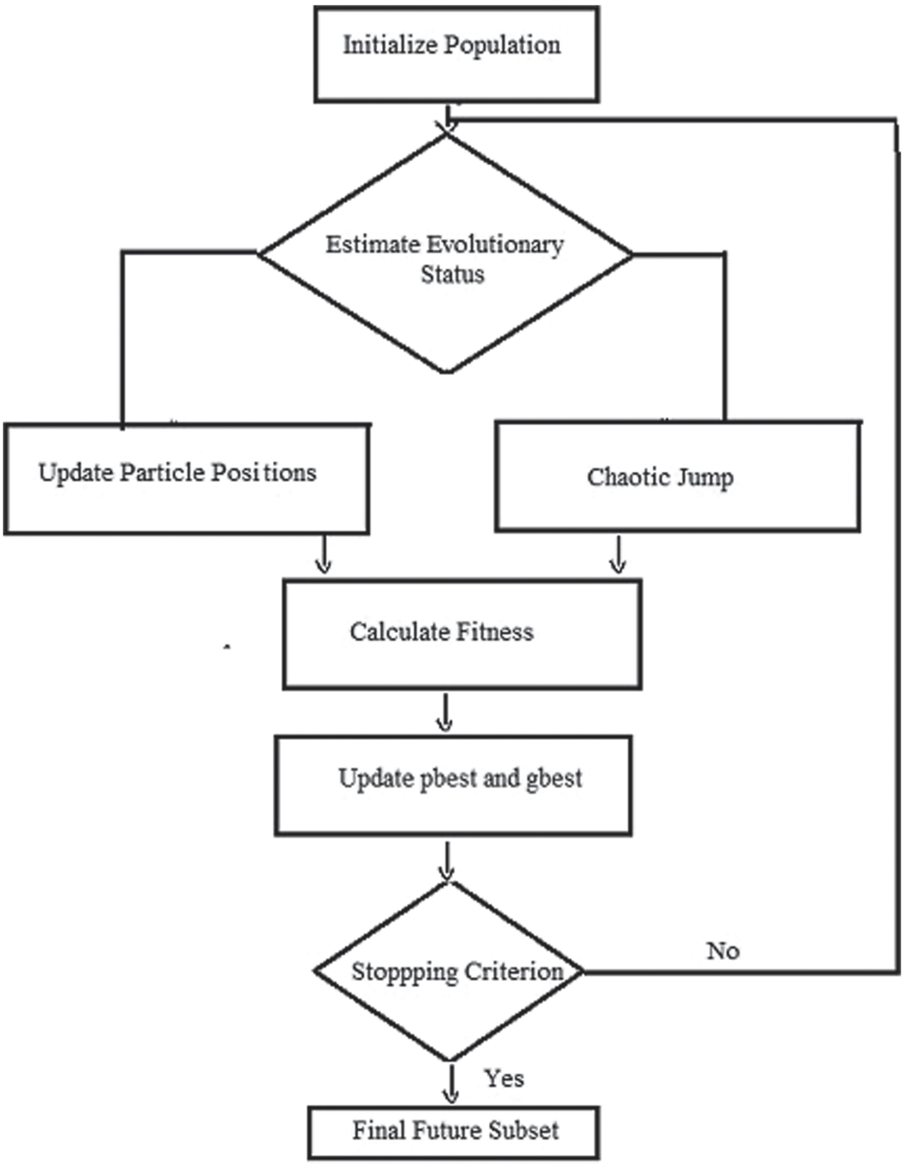

Figure 3. Flow chart for the proposed algorithm.

the limit for each particle so that a particle never violates the position limit in any dimension.

Step 9: check whether the best solution is greater than a pre-specified number or the number of iterations reaches the maximum iteration, then stop the process, otherwise go to *Step 3*.

3.3. Fitness-objective function evaluation

The ultimate goal of this work is to trim down the frequency deviation and tie-line power flow deviations. The performance criterion (ITAE) is also implemented to improve the dynamics of AGC in a proposed test system.

The fitness function

$$\int_0^{tsim} t|e(t)|dt \tag{15}$$

where $e(t)$ is the error considered.

Minimization of fitness function:

$$j = \int_0^{tsim} (\beta_1|\Delta f_1| + \beta_2|\Delta f_2| + |\Delta p_{\text{tie}12}^{\text{error}}|)dt + FD \tag{16}$$

where $\text{FD} = \alpha_1\text{OS} + \alpha_2\text{ST}$; OS is the Over Shoot; ST is the Settling Time.

The comparison between the performance criterion for the proposed controller along with RCGA-based PI and DE-based PI are presented in Table 3. Figure 3 shows the Flow chart for the proposed algorithm.

Table 4. Actual power generated (pu).

Area	Genco	Scenario 1	Scenario 2	Scenario 3
1	1	0.1	0.09	0.107
	2	0.04	0.085	0.097
	3	0.075	0.09	0.11
2	1	0.042	0.065	0.075
	2	0.09	0.085	0.1
3	1	0.05	0.09	0.105
	2	0.06	0.06	0.068
4	1	0.125	0.05	0.07
	2	0.058	0.02	0.03
5	1	0.11	0.1	0.11
	2	0.045	0.065	0.0825

4. Results and discussion

Here, the five areas deregulated system for thermal generation are simulated through Matlab Simulink. Three possible contracted test scenarios are considered for validating the robustness of the proposed control strategy against parametric uncertainties; the simulations are carried out for large load demands . The plant and control parameters for the test system are presented as supporting information in Tables 1 and 2. To illustrate the staunchness of the BBPSO-PI controller, the responses of RCGA-PI [19] and DE–PI controller have also been compared. The actual power generated is represented in Table 4. Tables 5 and 6 depicted the frequency and tie-line power flow deviations of the test system.

4.1. Scenario 1 pool co-based transactions

The Gencos can deliver load following within their control areas based on the agreement, this case of pool co-based contracts between Discos and available Gencos is simulated based on the AGPM given below.

$$\text{AGPM} = \begin{pmatrix} 0 & 0 & 0.3 & 0 & 0.1 & 0.2 & 0 & 0.3 \\ 0.5 & 0 & 0 & 0.2 & 0 & 0.1 & 0.1 & 0 \\ 0 & 0.3 & 0 & 0 & 0.25 & 0.1 & 0.1 & 0 \\ 0.25 & 0.2 & 0.4 & 0 & 0 & 0 & 0 & 0 \\ 0 & 0.25 & 0.1 & 0.25 & 0 & 0 & 0 & 0 \\ 0 & 0 & 0.2 & 0.2 & 0.5 & 0 & 0 & 0 \\ 0 & 0 & 0 & 0.35 & 0.15 & 0 & 0 & 0 \\ 0 & 0.25 & 0 & 0 & 0 & 0.4 & 0 & 0 \\ 0 & 0 & 0 & 0 & 0 & 0.2 & 0 & 0 \\ 0.25 & 0 & 0 & 0 & 0 & 0 & 0.6 & 0 \\ 0 & 0 & 0 & 0 & 0 & 0 & 0.3 & 0.7 \end{pmatrix}$$

Table 5. Frequency deviation.

		Frequency deviation (p.u. Hz)								
		Overshoots (p.u. Hz)			Undershoots (p.u. Hz)			Settling time (secs)		
Scenario	Area	BBPSO-PI	RCGA-PI	DE-PI	BBPSO-PI	RCGA-PI	DE-PI	BBPSO-PI	RCGA-PI	DE-PI
1	1	0.013873	4.13E-02	0.036523	−0.1061	−1.06E-01	−0.10605	4.5	5.2	4.6
	2	0.005082	1.87E-02	0.006581	−0.04324	−3.81E-02	−0.03607	4.6	4.8	4.7
	3	0.065028	1.44E-01	0.09606	−0.1516	−1.62E-01	−0.15156	3.3	5.1	3.8
	4	0.004837	1.05E-02	0.020462	−0.0419	−4.89E-02	−0.05635	3.8	4.5	4.4
	5	0.061571	6.03E-02	0.036558	−0.11701	−1.17E-01	−0.11701	3.8	5.8	4.1
2	1	1.22E-01	1.85E-01	0.1654305	−1.06E-01	−1.06E-01	−0.11599	4.3	4.8	4.5
	2	1.28E-01	7.01E-02	0.1018131	−3.77E-02	−3.60E-02	−0.03666	5.2	5.3	5.4
	3	9.97E-03	1.43E-02	0.0126948	−1.70E-01	−1.52E-01	−0.17094	7.1	7.9	7.2
	4	−1.45E-30	1.64E-04	8.27E-05	−5.30E-02	−4.43E-02	−0.05604	8.1	8.1	8.1
	5	2.43E-02	7.62E-03	0.0077144	−1.17E-01	−1.17E-01	−0.11724	6.1	6.3	6.2
3	1	1.41E-01	1.39E-01	1.71E-01	−1.53E-01	−1.53E-01	−1.53E-01	3.8	4.8	4.1
	2	8.04E-02	6.47E-02	9.94E-02	−4.83E-02	−4.84E-02	−4.84E-02	4.6	5.2	4.8
	3	1.27E-02	9.29E-02	1.31E-02	−2.12E-01	−2.97E-01	−2.05E-01	4.8	5.4	4.9
	4	−1.74E-30	−1.14E-05	−1.74E-30	−5.55E-02	−5.69E-02	−5.21E-02	8.2	9.1	10
	5	2.37E-02	0.004252	7.53E-06	−1.48E-01	−1.48E-01	−1.48E-01	3.8	4.4	4.1

Table 6. Inter-area tie-line power flow deviations.

		Tie-line power deviations (pu Mw)								
		Overshoots			Undershoots			Settling time		
Scenario	Area	BBPSO-PI	RCGA-PI	DE-PI	BBPSO-PI	RCGA-PI	DE-PI	BBPSO-PI	RCGA-PI	DE-PI
1	1&2	2.79E-03	0.009747	0.00636	−2.10E-03	−0.00375	−0.00212	4.6	6.8	3.2
	1&3	6.67E-03	0.007169	0.007083	−2.28E-04	−0.00354	−0.00212	4.9	5.8	4.8
	1&4	4.24E-06	0.008425	0.001742	−8.44E-03	−0.01428	−0.0102	5.1	5.2	5.2
	2&3	1.31E-03	0.001051	0.000964	−2.37E-06	−0.00016	−0.00036	12.1	8.9	14.1
	1&5	8.01E-04	0.000769	0.000276	−9.26E-04	−0.00171	−0.00172	9.9	8.6	14.1
2	1&2	4.82E-02	0.047729	5.08E-02	−1.93E-03	−0.00221	−0.00295	4.1	5.2	4.6
	1&3	4.50E-02	0.048619	0.045006	1.49E-60	0	0	4.1	5.2	4.1
	1&4	−7.51E-61	0	0	−6.57E-02	−0.06947	−0.06656	5.1	5.2	5.2
	2&3	1.01E-03	0.001114	0.001324	−1.50E-02	−0.01513	−0.01507	7.1	7.2	7.2
	1&5	1.21E-04	0.00012	0.000176	−1.50E-02	−0.01499	−0.01499	6.2	6.3	6.3
3	1&2	4.82E-02	0.048406	0.050453	−4.59E-03	−0.00369	−0.00479	3.8	4.2	4.8
	1&3	4.50E-02	0.047756	0.045	1.86E-60	0	0	3.6	5.4	3.7
	1&4	−8.28E-61	0	0	−6.65E-02	−0.07104	−6.83E-02	4.8	6.1	5.1
	2&3	2.07E-03	0.002074	0.002231	−1.50E-02	−0.015	−0.015	5.2	5.6	5.3
	1&5	3.97E-04	0.000399	0.000401	−1.50E-02	−0.01502	−0.01501	10.1	10.2	10.3

4.2. Scenario 2 combination of pool-co and bilateral-based transactions

This case reveals the bilateral cum poolco-based transaction between Dicos and Gencos. In this power transaction of the deregulated system, Discos have full freedom of demanding power from any of Genco within or with other control areas as per agreement. The following AGPM shows the transactions between the areas.

$$\mathrm{AGPM} = \begin{pmatrix} 0 & 0 & 0.3 & 0 & 0.1 & 0.2 & 0 & 0.3 \\ 0.5 & 0 & 0 & 0.2 & 0 & 0.1 & 0.1 & 0 \\ 0 & 0.3 & 0 & 0 & 0.25 & 0.1 & 0.1 & 0 \\ 0.25 & 0.2 & 0.4 & 0 & 0 & 0 & 0 & 0 \\ 0 & 0.25 & 0.1 & 0.25 & 0 & 0 & 0 & 0 \\ 0 & 0 & 0.2 & 0.2 & 0.5 & 0 & 0 & 0 \\ 0 & 0 & 0 & 0.35 & 0.15 & 0 & 0 & 0 \\ 0 & 0.25 & 0 & 0 & 0 & 0.4 & 0 & 0 \\ 0 & 0 & 0 & 0 & 0 & 0.2 & 0 & 0 \\ 0.25 & 0 & 0 & 0 & 0 & 0 & 0.6 & 0 \\ 0 & 0 & 0 & 0 & 0 & 0 & 0.3 & 0.7 \end{pmatrix}$$

4.3. Scenario 3 contract violations

In this power transaction, it is assumed that Discos demanding power by violating the contract. The main objective of framing this case is to reveal the robustness of the proposed controller. Since the Discos violated the contracts as made with Gencos, the excessive loads demanded by each of various areas are as follows area 1, area 2, area 3, area 4 and area 5 are 0.050, 0.0200, 0.0400, 0.0200 and 0.0300, p.u respectively. The responses of frequency and tie-line deviations are shown in Figures 4–8. The Gencos are following the AGPM of Case 2 in this transaction.

The simulation results show that the proposed BBPSO-PI controller pursues the change in demand and overwhelming robust performance for a broad range of disturbances in load and possible contracted scenarios in the presence of GRC compared to RCGA-PI and DE-PI controller.

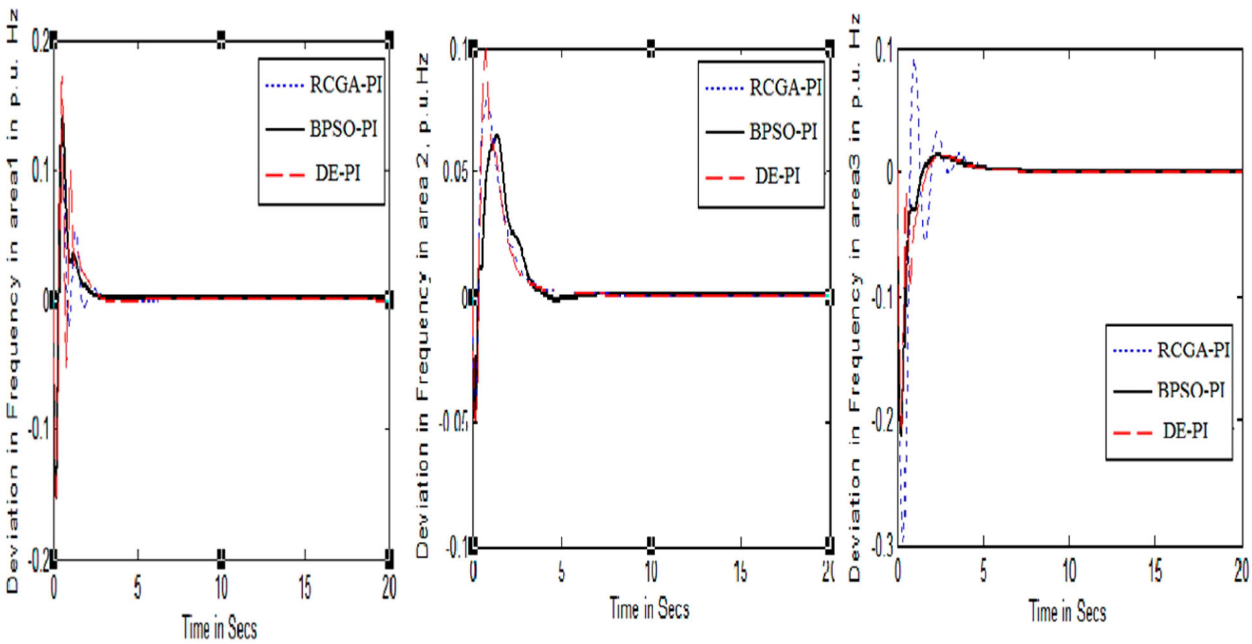

Figure 4. Frequency deviations of area 1, area 2 & area 3 for scenario 3.

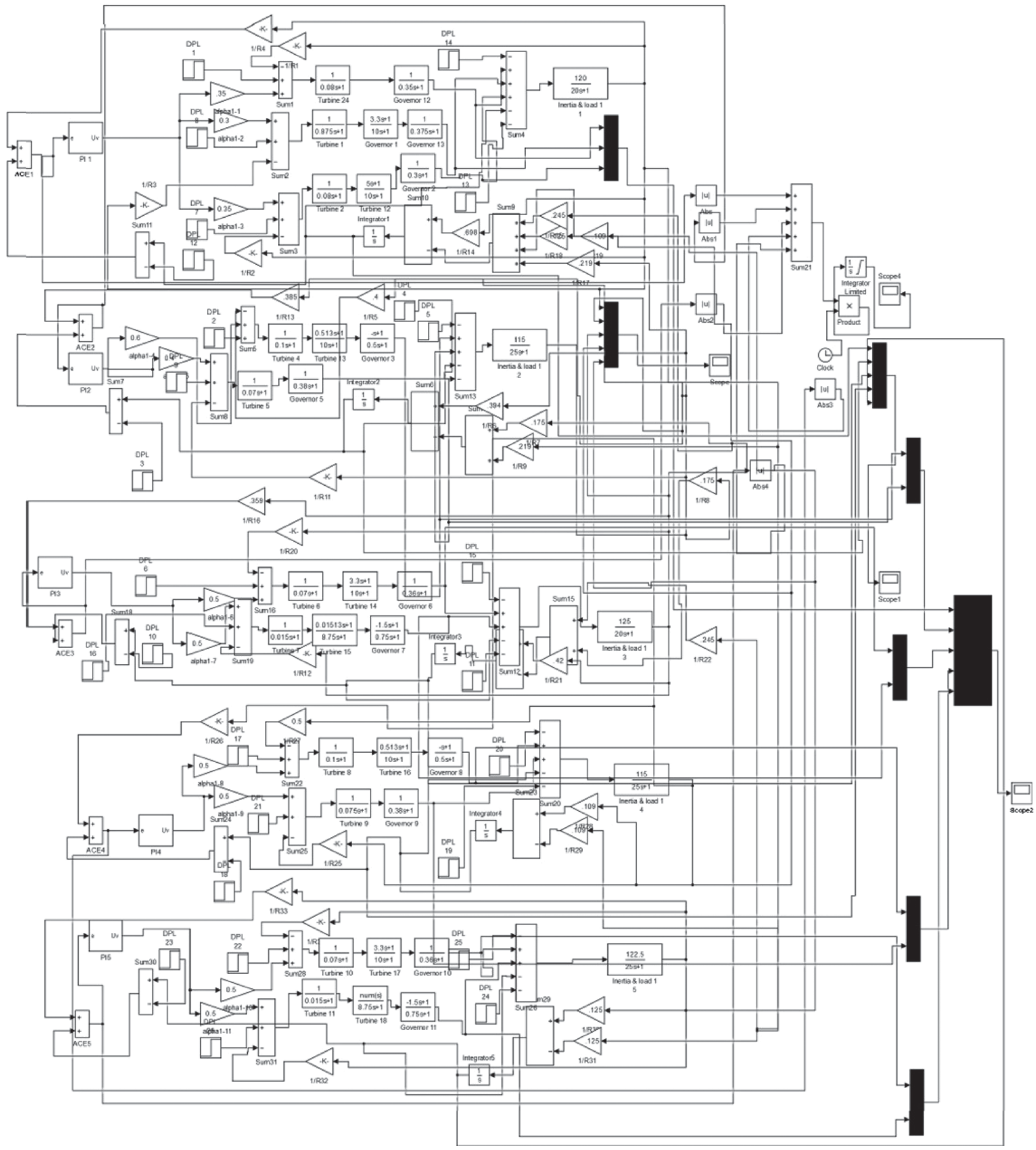

Figure 5. Simulink model for the five-area thermal deregulated power system.

5. Conclusions

The primary motto of this work is to reveal the robustness of the BBPSO algorithm whose gain is tuned through the PI controller against AGC to regulate area control error to zero. Five area control structures of deregulated power systems are considered test environments. To manifest the designed controller, the test control area of the thermal generation restructured power system is considered with generation rate constraint. The novelty of the designed controller is proven through the simulation results. The simulation has been done through Matlab Simulink for three cases. The robust performances have been revealed by comparing the proposed controller with RCGA-PI and DE-PI controllers. From the dynamic performances, it is proved that the proposed controller holds good for various contracted scenarios and in the presence of large disturbances. It reflects robustness in reduced overshoots, undershoots and settling time in their transient response. However, the controller exhibits simple architecture and can handle real-time environments but they lag in their computational time hence to reduce, AI Techniques may be implemented in future work.

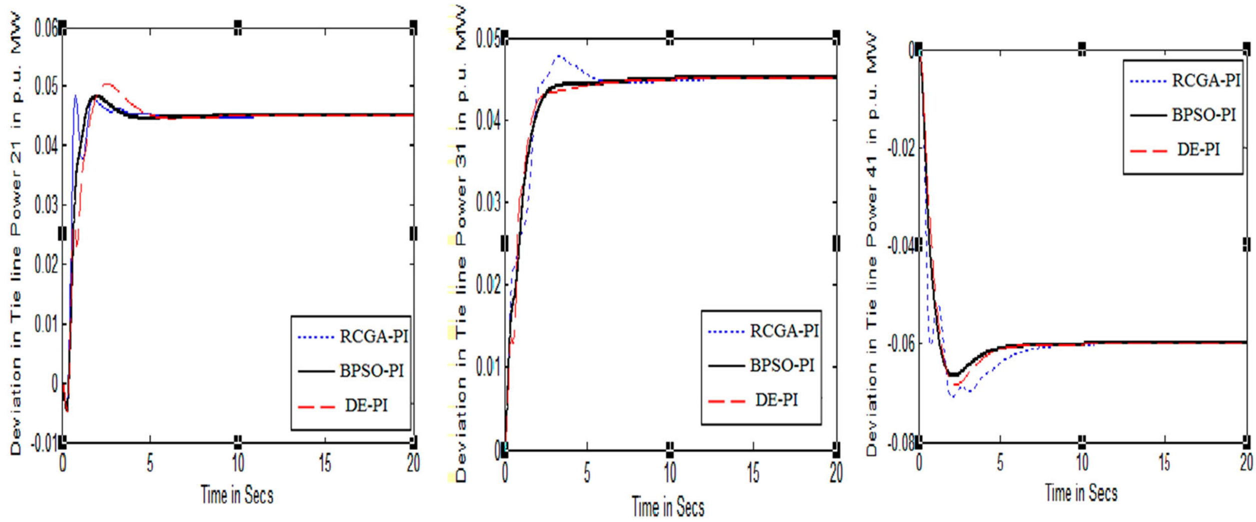

Figure 6. Frequency deviations of area 4 & area 5 for scenario 3.

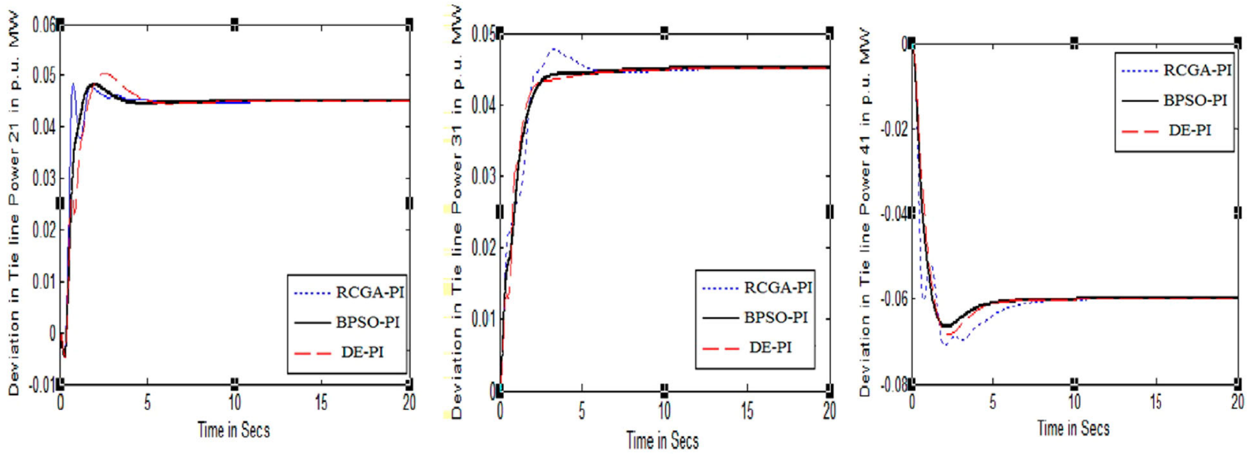

Figure 7. Tie-line power deviations between areas 2 & 1, 3 & 1 and 4 & 1 for scenario 3.

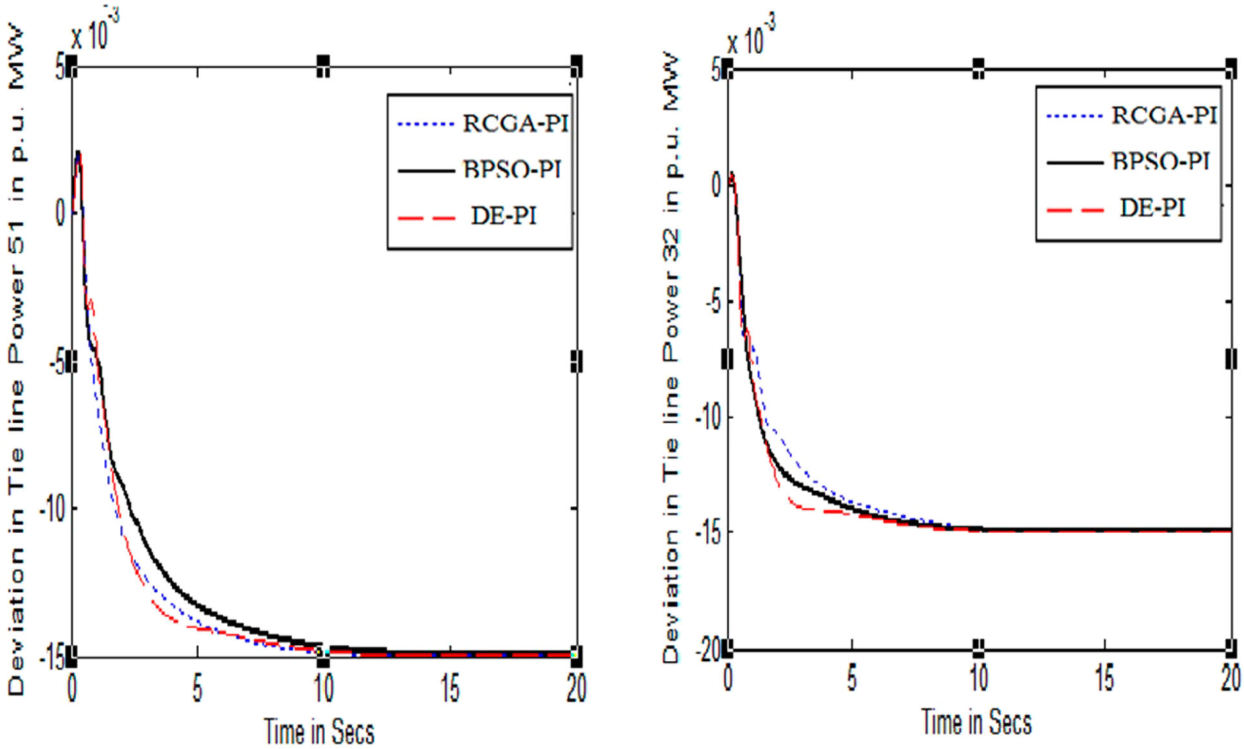

Figure 8. Tie-line power deviations between areas 5 & 1 and 3 & 2 for scenario 3.

Nomenclature

i	subscript referred to the area
F	Area frequency
P_{tie}	tie-line power flow
ACE	area control error
cpf	contract participation factor
gpf	generation participation factor
K_P	subsystem equivalent gain constant
T_P	subsystem equivalent time constant
T_T	turbine time constant
T_G	governor time constant
B	frequency bias
T_{ij}	tie-line synchronizing coefficient between areas i & j
Pd	area load disturbance
P_{Lji}	contracted demand of DISCO j in area i
P_{ULji}	un-contracted demand of DISCO j in area i
$P_{M,ji}$	power generation of GENCO j in area i
P_{Loc}	total local demand
η	Area interface
ξ	Scheduled power tie-line power flow deviation

Disclosure statement

No potential conflict of interest was reported by the author(s).

References

[1] Akash Monohar J. A systematic study of controller and optimization techniques in automatic generation control system. 2023 International Conference on Computational Intelligence, Communication Technology and Networking (CICTN), Ghaziabad. IEEE; 2023. p. 339–343.

[2] Pati TK, Sahu BK. Application of hybrid DEPSO algorithm to study the performance of different PID controller structures for automatic generation control of a two-area multi-units interconnected power system. 2014 International Conference on Circuit, Power and Computing Technologies [ICCPCT], Nagercoil. IEEE; 2014. p. 787–791.

[3] Sahoo G, Sahu RK, Panda S. Automatic generation control and its comparative analysis for interconnected thermal and hydrothermal power system by ERWCA optimization technique. 2023 International Conference on Intelligent and Innovative Technologies in Computing, Electrical and Electronics (IITCEE), Bengaluru. IEEE; 2023. p. 1106–1110.

[4] Khuntia SR. Comparative study of different controllers for automatic generation control of an interconnected hydro-thermal system with generation rate constraints. 2010 International Conference on Industrial Electronics, Control and Robotics, Rourkela. IEEE; 2010. p. 243–246.

[5] ShadanSalik S, NehaKhokher NK. Fuzzy logic based automatic generation control. Proceedings of the Fifth International Conference on Communication and Electronics Systems (ICCES 2020), Coimbatore. IEEE; 2020. p. 193–198.

[6] Behera A, Panigrahi TK. A novel cascaded PID controller for automatic generation control analysis with renewable sources. IEEE/CAA J Automat Sin. 2019;6(6):1438–1451. doi:10.1109/JAS.2019.1911666

[7] Mao J, Liu R, Aihua WU, et al. An improved whale optimization algorithm based PIDF–(1+PI) cascade automatic generation control for multi-area multi-source power system with capacitive energy storage. IEEE Access. 2023;11:72418–72435. doi:10.1109/ACCESS.2023.3250558

[8] LihuiXie JW, Li Y, Sun Q. Automatic generation control strategy for integrated energy system based on ubiquitous power internet of things. IEEE Internet Things J. 2023;10(9):7645–7654. doi:10.1109/JIOT.2022.3209792

[9] MuslehUddin M, Saifullah MK, MonirulKabir M. PID controller based automatic generation control for three area interconnected power system. 2021 International Conference on Information and Communication Technology for Sustainable Development (ICICT4SD), Dhaka. IEEE; 2021. p. 300–305.

[10] Liu Q, Liu Q. Research on automatic generation control system of photovoltaic power station based on adaptive PID control algorithm. 2020 IEEE 3rd International Conference on Information Systems and Computer Aided Education (ICISCAE), Dalian. 2020. p. 231–236.

[11] Kennedy J. Bare bones particle swarms. Proceedings of IEEE Swarm Intelligence Symposium (SIS'03), Indianapolis. IEEE; 2003. p. 80–87.

[12] Ali AM, Saad MS, Amari AE, et al. Automatic generation control of simplified Egyptian power system using fractional order PI controller based on PSO. Int J Energy Environ Sci. 2023;8(2):31–43.

[13] Kumar S, Gupta SK. Load frequency control of a two-area, multi-unit AGC hybrid power system under deregulated environment using PI-PDF and CPI-PDF tuner with differential evolution algorithm. Int J Intell Syst Appl Eng. 2024;12(4s):16–29.

[14] Kundur P. Power system stability and control. New York (NY): McGraw-Hill; 1994.

[15] Lal DK, Barisal AK, Tripathy M. Differential evolution algorithm optimized dual mode load frequency controller for isolated wind-diesel power system with SMES and fuel cell. Recent Adv Electric Electron Eng. 2019;12(1):56–61.

[16] Arya LD, Verma HK, Jain C. Differential evolution for optimization of PID gains in automatic generation control. Int J Comput Sci Eng. 2011;3(5):1848–1856.

[17] Ghoshal SP. Application of GA based optimal integral gains in fuzzy based active power-frequency control of non-reheat and reheat thermal generating systems. Electr Power Syst Res. 2003;67(2):79–88. doi:10.1016/S0378-7796(03)00087-7

[18] Bevrani H. Robust decentralised load-frequency control using an iterative linear matrix inequalities algorithm. IEE Proc Gener Transm Distrib. 2004;151(3):347–354. doi:10.1049/ip-gtd:20040493

[19] Demiroren A, Zeynelgil H L. GA application to optimization of AGC in three area power system after deregulation. Int. J. Electr. Power Energy Syst. 2007;29:230–240.